arXiv:cond-mat/0106209v1 [cond-mat.dis-nn] 12 Jun 2001

Statistical Mechanics of Linear Compression Codes in Network Communication

Tatsuto Murayama

Department of Computational Intelligence and Systems Science, Tokyo Institute of Technology - Yokohama 2268502, Japan

PACS. 89.90.+n – Other areas of general interest to physicists.
PACS. 89.70.+c – Information science.
PACS. 05.50.+q – Lattice theory and statistics; Ising problems.

Abstract. – We analyze the performance of a linear code used for a data compression of Slepian-Wolf type. In our framework, two correlated data are separately compressed into codewords employing Gallager-type codes and casted into a communication network through two independent input terminals. At the output terminal, the received codewords are jointly decoded by a practical algorithm based on the Thouless-Anderson-Palmer approach. Our analysis shows that the achievable rate region presented in the data compression theorem by Slepian and Wolf is described as first-order phase transitions among several phases. The typical performance of the practical decoder is also well evaluated by the replica method.

The ever increasing information transmission in the modern world is based on network communications. While a lot of cutting edge technologies have been developed to realize the comfortable communication, few techniques are designed for network-based data transmission. It is quite strange that even the up-to-date information technologies are based on point-to-point protocols, although the global computer network called 'the Internet' already exists. Therefore, now is the time that we focus on the multi terminal communication techniques.

Data compression, or source coding, is a scheme to reduce the size of message (data) in information representation. In his seminal paper [9], Shannon showed that for an information source represented by a distribution $\mathcal{P}(\boldsymbol{S})$ of N dimensional Boolean (binary) vector $\boldsymbol{S}$, one can employ another representation in which the message length N is reduced to $M(\leq N)$ without any distortion, if the code rate $R = M/N$ satisfies $R \geq H_2(\boldsymbol{S})$ in the limit $N,\ M \to \infty$. Here, $H_2(\boldsymbol{S}) = -(1/N)\,\mathrm{Tr}_{\boldsymbol{S}}\,\mathcal{P}(\boldsymbol{S})\log_2\mathcal{P}(\boldsymbol{S})$ represents the binary entropy per bit in the original representation $\boldsymbol{S}$ indicating the optimal compression rate.

Unfortunately, Shannon's theorem itself is non-constructive and does not provide explicit rules for devising the optimal codes. Therefore, it is surprising that a practical code proposed by Lempel and Ziv (LZ) in 1973 [14] saturates the Shannon's optimal compression limit in the case of point-to-point communication. However, it should be emphasized here that generalization of the LZ codes to advanced data compression suitable for network communications (NC) is difficult although importance of the NC is rapidly increasing as recent development of the Internet. This is mainly because all the practical codes that saturate Shannon's limit to

© EDP Sciences

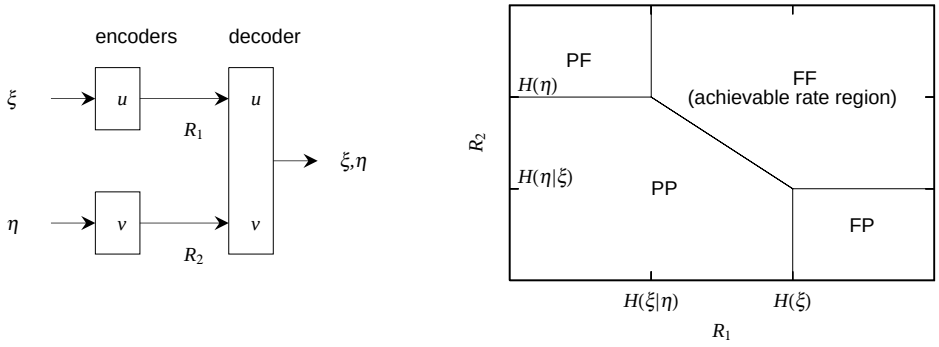

(a) Slepian and Wolf system

(b) Achievable rate region

Fig. 1 – (a)Slepian and Wolf system: A simple communication network introduced in the data compression theorem of Slepian and Wolf. Separate coding is assumed in the distributed system. (b) Achievable rate region: Code rates are classified into four categories according to whether the two compressed data are decodable or not. The parameter regime where the both data are decodable without any distortion is termed the *achievable rate region.*

date require a complete knowledge about all source vectors coming into the communication network while the compression should be carried out independently on each terminal in usual situations. Therefore, the quest for more efficient compression codes that are suitable for NC still remains one of the most important topics in information theory [1].

The purpose of this letter is to employ recent developments of the research on error-correcting codes (ECC) for this purpose. More specifically, we will investigate the efficacy and the limitation of a linear compression scheme inspired by Gallager's ECC [2], which has been actively investigates in both of information theory and physics communities [4–6, 8], when it is applied to a data compression problem introduced by Slepian and Wolf (SW) in the research of NC [10]. Unlike the existing argument in information theory, our approach based on statistical mechanics makes it possible not only to assess the theoretical bounds of the achievable performance but also to provide practical encoding/decoding methods that can be performed in linear time scales with respect to the data length.

Let us start with setting up the framework of the SW problem [10]. In a general scenario, two correlated N-dimensional Boolean vectors $\boldsymbol{\xi}$ and $\boldsymbol{\eta}$ are *independently* compressed to M-dimensional vectors $\boldsymbol{x}$ and $\boldsymbol{y}$ respectively. These compressed data (or codewords) $\boldsymbol{x}$ and $\boldsymbol{y}$ are decoded to retrieve the original data simultaneously by a single decoder. A schematic representation of this system is shown in Fig. 1(a).

The codes used in this letter are composed of randomly selected sparse matrices A and B of dimensionality $M_1 \times N$ and $M_2 \times N$, respectively. These are constructed similarly to those of Gallager's ECC [2] as being characterized by K_1 and K_2 nonzero unit elements per row and C_1 and C_2 nonzero unit elements per column, respectively. The compression rates can be different between the two terminals. Corresponding to matrices A and B, the rates are defined as $R_1 = M_1/N = K_1/C_1$ and $R_2 = M_2/N = K_2/C_2$, respectively. While both matrices are known to decoder, encoders only need to know their own matrix, that is, encoding carried out separately in this scheme as $\boldsymbol{u} = A\boldsymbol{\xi}$ and $\boldsymbol{v} = B\boldsymbol{\eta}$, where Boolean arithmetics are employed

to the Boolean vectors. After receiving the codewords $\boldsymbol{u}$ and $\boldsymbol{v}$, the couple of equations

$$\boldsymbol{u} = A\boldsymbol{S}, \quad \boldsymbol{v} = B\boldsymbol{\tau} \tag{1}$$

should be solved with respect to $\boldsymbol{S}$ and $\boldsymbol{\tau}$ which become the estimates of the original data $\boldsymbol{\xi}$ and $\boldsymbol{\eta}$, respectively.

To facilitate the current investigation we first map the problem to that of an Ising model with finite connectivity. We employ the binary representation $(+1, -1)$ of the dynamical variables $\boldsymbol{S}$ and $\boldsymbol{\tau}$ and of the vectors $\boldsymbol{u}$ and $\boldsymbol{v}$ rather than the Boolean $(0, 1)$ one; the vector $\boldsymbol{u}$ is generated by taking products of the relevant binary data bits $u_{\langle i_1, i_2, \cdots, i_{K_1}\rangle} = \xi_{i_1}\xi_{i_2}\cdots\xi_{i_{K_1}}$, where the indices $i_1, i_2, \cdots, i_{K_1}$ correspond to the nonzero elements of A, producing a binary version of $\boldsymbol{u}$, and similarly for $\boldsymbol{v}$. Assuming the thermodynamic limit $N,\ M_1,\ M_2 \to \infty$ keeping the code rates $R_1 = M_1/N$ and $R_2 = M_2/N$ finite is quite natural as communication to date generally requires transmitting large data, where finite size corrections are likely to be negligible. To explore the system's capabilities we examine the partition function

$$\begin{aligned} \mathcal{Z} = \operatorname*{Tr}_{\boldsymbol{S},\boldsymbol{\tau}} \mathcal{P}(\boldsymbol{S},\boldsymbol{\tau}) & \prod_{\langle i_1, i_2, \cdots, i_{K_1}\rangle} \left[1 + \frac{1}{2}\mathcal{A}_{\langle i_1, i_2, \cdots, i_{K_1}\rangle}\left(u_{\langle i_1, i_2, \cdots, i_{K_1}\rangle} \cdot S_{i_1}S_{i_2}\cdots S_{i_{K_1}} - 1\right)\right] \\ & \times \prod_{\langle i_1, i_2, \cdots, i_{K_2}\rangle} \left[1 + \frac{1}{2}\mathcal{B}_{\langle i_1, i_2, \cdots, i_{K_2}\rangle}\left(v_{\langle i_1, i_2, \cdots, i_{K_2}\rangle} \cdot \tau_{i_1}\tau_{i_2}\cdots\tau_{i_{K_2}} - 1\right)\right]. \end{aligned} \tag{2}$$

The tensor product $\mathcal{A}_{\langle i_1, i_2, \cdots, i_{K_1}\rangle} u_{\langle i_1, i_2, \cdots, i_{K_1}\rangle}$, where $u_{\langle i_1, i_2, \cdots, i_{K_1}\rangle} = \xi_{i_1}\xi_{i_2}\cdots\xi_{i_{K_1}}$ is the binary equivalent of $A\boldsymbol{\xi}$. Elements of the sparse connectivity tensor $\mathcal{A}_{\langle i_1, i_2, \cdots, i_{K_1}\rangle}$ take the value 1 if the corresponding indices of data are chosen (i.e., if all corresponding indices of the matrix A are 1) and 0 otherwise; it has C_1 unit elements per i index representing the system's degree of connectivity. Notice that if the product $S_{i_1}S_{i_2}\cdots S_{i_{K_1}}$ is in disagreement with the corresponding element $u_{\langle i_1, i_2, \cdots, i_{K_1}\rangle}$, which implies an error for the parity check, the value of the partition function $\mathcal{Z}$ vanishes. Similar arguments are valid for $\mathcal{B}_{\langle i_1, i_2, \cdots, i_{K_2}\rangle}$ and $v_{\langle i_1, i_2, \cdots, i_{K_2}\rangle}$. The probability $\mathcal{P}(\boldsymbol{S},\boldsymbol{\tau})$ represents our prior knowledge of data including the correlation between the sources $\boldsymbol{\xi}$ and $\boldsymbol{\eta}$. Note that the dynamical variables $\boldsymbol{\tau}$, introduced to estimate $\boldsymbol{\eta}$, are irrelevant to the performance measure with respect to the other data $\boldsymbol{\xi}$.

Since the partition function Eq. (2) is invariant under the transformations $S_i \to S_i\xi_i$, $\tau_i \to \tau_i\eta_i$, $u_{\langle i_1, i_2, \cdots, i_{K_1}\rangle} \to u_{\langle i_1, i_2, \cdots, i_{K_1}\rangle}\xi_{i_1}\xi_{i_2}\cdots\xi_{i_{K_1}} = 1$ and $v_{\langle i_1, i_2, \cdots, i_{K_2}\rangle} \to v_{\langle i_1, i_2, \cdots, i_{K_2}\rangle}\tau_{i_1}\tau_{i_2}\cdots\tau_{i_{K_2}} = 1$, it is useful to decouple the correlations between the vectors $\boldsymbol{S}$, $\boldsymbol{\tau}$ and $\boldsymbol{\xi}$, $\boldsymbol{\eta}$. Rewriting Eq. (2) using this gauge, one obtains a similar expression apart from the first factor which becomes $\mathcal{P}(\boldsymbol{S}\otimes\boldsymbol{\xi}, \boldsymbol{\tau}\otimes\boldsymbol{\eta})$, where $\boldsymbol{S}\otimes\boldsymbol{\xi} = (S_i\xi_i)$ and $\boldsymbol{\tau}\otimes\boldsymbol{\eta} = (\tau_i\eta_i)$ for $i = 1, 2, \ldots, N$.

The random selection of elements in $\mathcal{A}$ and $\mathcal{B}$ indroduces disorder to the system; we average the logarithm of the partition function $\mathcal{Z}(\mathcal{A}, \mathcal{B}, \boldsymbol{u}, \boldsymbol{v})$ over the disorder and the statistical properties of both data, using the replica method [13]. In the calculation, a set of order parameters $q_{\alpha,\beta,\cdots,\gamma} = \frac{1}{N}\sum_{i=1}^{N} Z_i S_i^{\alpha} S_i^{\beta}\cdots S_i^{\gamma}$ and $r_{\alpha,\beta,\cdots,\gamma} = \frac{1}{N}\sum_{i=1}^{N} Y_i \tau_i^{\alpha}\tau_i^{\beta}\cdots\tau_i^{\gamma}$ arise, where $\alpha, \beta, \cdots, \gamma$ represent replica indices, and the variables Z_i and Y_i come from enforcing the restriction of C_1 and C_2 connections per index, respectively as in [6].

To proceed further, we have to make an assumption about the order parameters' symmetry. The assumption made here, and validated later on, is that of replica symmetry in the following representation of the order parameters and the related conjugate variables:

$$\begin{aligned} q_{\alpha,\beta,\cdots,\gamma} &= a_q \int dx\, \pi(x) x^l, \quad \widehat{q}_{\alpha,\beta,\cdots,\gamma} = a_{\widehat{q}} \int d\widehat{x}\, \widehat{\pi}(\widehat{x})\widehat{x}^l, \\ r_{\alpha,\beta,\cdots,\gamma} &= a_r \int dy\, \rho(y) y^l, \quad \widehat{r}_{\alpha,\beta,\cdots,\gamma} = a_{\widehat{r}} \int d\widehat{y}\, \widehat{\rho}(\widehat{y})\widehat{y}^l, \end{aligned} \tag{3}$$

where l is the number of replica indices and a_* are normalization factors to make $\pi(x)$, $\widehat{\pi}(\widehat{x})$, $\rho(y)$ and $\widehat{\rho}(\widehat{y})$ represent probability distributions. Unspecified integrals are carried out over the range $[-1,+1]$.

Extremizing the averaged expression with respect to the probability distributions, we obtain the following free energy per spin:

$$\begin{aligned}
\mathcal{F} &= -\frac{1}{N}\langle \ln \mathcal{Z}\rangle_{\mathcal{A},\mathcal{B},\mathcal{P}} \\
&= -\operatorname*{Extr}_{\pi,\widehat{\pi},\rho,\widehat{\rho}} \left\{ \frac{C_1}{K_1}\left\langle \ln\left(\frac{1+\prod_{i=1}^{K_1} x_i}{2}\right)\right\rangle_{\pi} + \frac{C_2}{K_2}\left\langle \ln\left(\frac{1+\prod_{i=1}^{K_2} y_i}{2}\right)\right\rangle_{\rho} \right. \\
&\quad -C_1\left\langle \ln\left(\frac{1+x\widehat{x}}{2}\right)\right\rangle_{\pi,\widehat{\pi}} - C_2\left\langle \ln\left(\frac{1+y\widehat{y}}{2}\right)\right\rangle_{\rho,\widehat{\rho}} \\
&\quad \left. +\frac{1}{N}\left\langle \ln\left[\operatorname*{Tr}_{\boldsymbol{S},\boldsymbol{\tau}} \prod_{i=1}^{N}\prod_{\mu=1}^{C_1}\left(\frac{1+\widehat{x}_{\mu i}S_i}{2}\right)\prod_{i=1}^{N}\prod_{\mu=1}^{C_2}\left(\frac{1+\widehat{y}_{\mu i}\tau_i}{2}\right)\mathcal{P}(\boldsymbol{S}\otimes\boldsymbol{\xi},\boldsymbol{\tau}\otimes\boldsymbol{\eta})\right]\right\rangle_{\widehat{\pi},\widehat{\rho},\mathcal{P}} \right\}, \qquad (4)
\end{aligned}$$

where the brackets with the subscript π and $\widehat{\pi}$ represent averages over the probability distributions $\pi(x)$ and $\pi(\widehat{x})$ with respect to variables denoted by x and $\widehat{x}$ with and without subscripts, respectively. Similar notations are also used for ρ and $\widehat{\rho}$. The bracket with the subscript $\mathcal{P}$ denotes the average with respect to $\boldsymbol{\xi}$ and $\boldsymbol{\eta}$ following the data distribution $\mathcal{P}(\boldsymbol{\xi},\boldsymbol{\eta})$.

Taking the functional derivative with respect to the distributions π, $\widehat{\pi}$, ρ and $\widehat{\rho}$, we obtain the following saddle point equations:

$$\begin{aligned}
\pi(x) &= \frac{1}{N}\sum_{i=1}^{N}\left\langle \delta\left[x-\tanh\left(F_i(\widehat{x}_{\mu j\in\mathcal{L}(\mu)/i},\widehat{y}_{\mu i};\boldsymbol{\xi},\boldsymbol{\eta})\xi_i + \sum_{\mu=1}^{C_1-1}\tanh^{-1}(\widehat{x}_{\mu i})\right)\right]\right\rangle_{\widehat{\pi},\widehat{\rho},\mathcal{P}} \\
\widehat{\pi}(\widehat{x}) &= \left\langle \delta\left(\widehat{x}-\prod_{i=1}^{K_1-1} x_i\right)\right\rangle_{\pi} \qquad (5)
\end{aligned}$$

where the effective fields denoted by F_i with subscripts are implicitly defined as

$$\begin{aligned}
&\frac{e^{F_i(\widehat{x}_{\mu j\in\mathcal{L}(\mu)/i},\widehat{y}_{\mu i};\boldsymbol{\xi},\boldsymbol{\eta})\xi_i S_i}}{2\cosh F_i(\widehat{x}_{\mu j\in\mathcal{L}(\mu)/i},\widehat{y}_{\mu i};\boldsymbol{\xi},\boldsymbol{\eta})} \\
&= \frac{\operatorname*{Tr}_{\boldsymbol{S}/S_i,\boldsymbol{\tau}} \prod_{j\in\mathcal{L}(\mu)/i}\prod_{\mu=1}^{C_1}\left(\frac{1+\widehat{x}_{\mu j}S_j}{2}\right)\prod_{i=1}^{N}\prod_{\mu=1}^{C_2}\left(\frac{1+\widehat{y}_{\mu i}\tau_i}{2}\right)\mathcal{P}(\boldsymbol{S}\otimes\boldsymbol{\xi},\boldsymbol{\tau}\otimes\boldsymbol{\eta})}{\operatorname*{Tr}_{\boldsymbol{S},\boldsymbol{\tau}} \prod_{i}^{N}\prod_{\mu=1}^{C_1}\left(\frac{1+\widehat{x}_{\mu i}S_i}{2}\right)\prod_{i=1}^{N}\prod_{\mu=1}^{C_2}\left(\frac{1+\widehat{y}_{\mu i}\tau_i}{2}\right)\mathcal{P}(\boldsymbol{S}\otimes\boldsymbol{\xi},\boldsymbol{\tau}\otimes\boldsymbol{\eta})}, \qquad (6)
\end{aligned}$$

and similarly for $\rho(y)$ and $\widehat{\rho}(\widehat{y})$. Notice that the notation $\boldsymbol{S}/S_i$ represents the set of all dynamical variables $\boldsymbol{S}$ except S_i. On the other hand, $\mathcal{L}_1(\mu)$ and $\mathcal{L}_2(\mu)$ denote the set of all indices of nonzero components in the μth row of A and B, respectively. The notation $\mathcal{L}_1(\mu)/i$ represents the set of all indices belonging to $\mathcal{L}_1(\mu)$ except i, and similarly for others.

After solving these equations, the expectation of the overlap can be evaluated as

$$\mathsf{m}_1 = \frac{1}{N}\left\langle \sum_{i=1}^{N}\xi_i \operatorname{sign}\langle S_i\rangle\right\rangle_{\mathcal{A},\mathcal{P}} = \int dz\,\phi(z)\operatorname{sign}(z), \qquad (7)$$

where we denote thermal averages $\langle \cdots \rangle$ and

$$\phi(z) = \frac{1}{N}\sum_{i=1}^{N}\left\langle \delta\left[z - \tanh\left(F_i(\widehat{x}_{\mu j\in\mathcal{L}(\mu)/i}, \widehat{y}_{\mu i}; \boldsymbol{\xi}, \boldsymbol{\eta})\xi_i + \sum_{i=1}^{C_1} \tanh^{-1}\widehat{x}_i \right) \right] \right\rangle_{\widehat{\pi},\widehat{\rho},\mathcal{P}}, \tag{8}$$

and similarly for m_2 of the overlap between $\boldsymbol{\eta}$ and its estimator.

The performance of the current compression method can be measured by the vector $\mathbf{m} = (\mathsf{m}_1, \mathsf{m}_2)$. Hereafter, we use the term 'ferromagnetic' to specify the perfect retrieval, that is , $\mathsf{m}_1 = 1$ (or $\mathsf{m}_2 = 1$), while the term 'paramagnetic' implies the distortion, that is, $\mathsf{m}_1 < 1$ (or $\mathsf{m}_2 < 1$). For instance, a term such as 'ferromagnetic-paramagnetic phase' denotes the phase characterized by the performance vector $\mathbf{m} \in \{(\mathsf{m}_1, \mathsf{m}_2) | \mathsf{m}_1 = 1, \mathsf{m}_2 < 1\}$, and so on.

One can show that the ferromagnetic-ferromagnetic state (FF): $\pi(x) = \delta(x-1),\ \widehat{\pi}(\widehat{x}) = \delta(\widehat{x}-1),\ \rho(y) = \delta(y-1)$ and $\widehat{\rho}(\widehat{y}) = \delta(\widehat{y}-1)$ always satisfies Eq. (5). In addition, in the limit of $C_1,\ C_2 \to \infty$, four solutions describing the paramagnetic-paramagnetic state (PP): $\pi(x) = \delta(x),\ \widehat{\pi}(\widehat{x}) = \delta(\widehat{x}),\ \rho(y) = \delta(y)$ and $\widehat{\rho}(\widehat{y}) = \delta(\widehat{y})$, the paramagnetic-ferromagnetic phase (PF): $\pi(x) = \delta(x),\ \widehat{\pi}(\widehat{x}) = \delta(\widehat{x}),\ \rho(y) = \delta(y-1)$ and $\widehat{\rho}(\widehat{y}) = \delta(\widehat{y}-1)$ and the ferromagnetic-paramagnetic state (FP): $\pi(x) = \delta(x-1),\ \widehat{\pi}(\widehat{x}) = \delta(\widehat{x}-1),\ \rho(y) = \delta(y)$ and $\widehat{\rho}(\widehat{y}) = \delta(\widehat{y})$ are also analytically obtained for an *arbitrary* joint distribution $\mathcal{P}(\boldsymbol{\xi}, \boldsymbol{\eta})$. Free energies corresponding to these solutions are provided from Eq. (4) as

$$\begin{aligned}
\mathcal{F}_{FF} &= -\frac{1}{N}\operatorname*{Tr}_{\boldsymbol{\xi},\boldsymbol{\eta}} \mathcal{P}(\boldsymbol{\xi}, \boldsymbol{\eta}) \ln \mathcal{P}(\boldsymbol{\xi}, \boldsymbol{\eta}),\ \mathcal{F}_{PP} = (R_1 + R_2)\ln 2, \\
\mathcal{F}_{FP} &= R_2 \ln 2 - \frac{1}{N}\operatorname*{Tr}_{\boldsymbol{\xi}} \mathcal{P}(\boldsymbol{\xi}) \ln \mathcal{P}(\boldsymbol{\xi}),\ \mathcal{F}_{PF} = R_1 \ln 2 - \frac{1}{N}\operatorname*{Tr}_{\boldsymbol{\eta}} \mathcal{P}(\boldsymbol{\eta}) \ln \mathcal{P}(\boldsymbol{\eta}),
\end{aligned} \tag{9}$$

where subscripts stand for corresponding states and $\mathcal{P}(\boldsymbol{\xi}) = \operatorname{Tr}_{\boldsymbol{\eta}} \mathcal{P}(\boldsymbol{\xi}, \boldsymbol{\eta})$ and $\mathcal{P}(\boldsymbol{\eta}) = \operatorname{Tr}_{\boldsymbol{\xi}} \mathcal{P}(\boldsymbol{\xi}, \boldsymbol{\eta})$ represent marginal distributions for the two source vectors $\boldsymbol{\xi}$ and $\boldsymbol{\eta}$, respectively.

Perfect decoding is theoretically possible if $\mathcal{F}_{FF}$ is the lowest among the above four. The corresponding parameter regime termed *achievable rate region* is shown in Fig. 1(b) as an intersection of the inequalities

$$R_1 + R_2 \geq H_2(\boldsymbol{\xi}, \boldsymbol{\eta}), \quad R_1 \geq H_2(\boldsymbol{\xi}|\boldsymbol{\eta}), \quad R_2 \geq H_2(\boldsymbol{\eta}|\boldsymbol{\xi}), \tag{10}$$

where $H_2(\boldsymbol{\xi}, \boldsymbol{\eta}) = -(1/N)\operatorname{Tr}_{\boldsymbol{\xi},\boldsymbol{\eta}} \mathcal{P}(\boldsymbol{\xi}, \boldsymbol{\eta}) \ln \mathcal{P}(\boldsymbol{\xi}, \boldsymbol{\eta})$, $H_2(\boldsymbol{\xi}|\boldsymbol{\eta}) = H_2(\boldsymbol{\xi}, \boldsymbol{\eta}) - H_2(\boldsymbol{\eta})$ and $H_2(\boldsymbol{\eta}|\boldsymbol{\xi}) = H_2(\boldsymbol{\xi}, \boldsymbol{\eta}) - H_2(\boldsymbol{\xi})$. It is worthy of noticing that this coincides with the achievable rate region saturated by the *optimal* data compression in the current framework previously shown by SW [10]. Namely, in the limit $C_1,\ C_2 \to \infty$, the current compression codes provide the optimal performance for *arbitrary* information sources $\mathcal{P}(\boldsymbol{\xi}, \boldsymbol{\eta})$.

For finite C_1 and C_2, the saddle point equations (5) can be solved numerically; but the properties of the system highly depend on the source distribution $\mathcal{P}(\boldsymbol{\xi}, \boldsymbol{\eta})$, which makes it difficult to go further without any assumption on the distribution. As a simple but non-trivial example, we will focus here on a component-wise correlated joint distribution

$$\mathcal{P}(\boldsymbol{S}, \boldsymbol{\tau}) = \prod_{i=1}^{N}\left(\frac{1 + m_1 S_i + m_2 \tau_i + q S_i \tau_i}{4} \right), \tag{11}$$

where a set of parameters m_1, m_2, and q characterize the data sources. To make Eq. (11) a distribution, these parameters must satisfy four inequalities $1 + m_1 + m_2 + q \geq 0$, $1 - m_1 + m_2 - q \geq 0$, $1 + m_1 - m_2 - q \geq 0$ and $1 - m_1 - m_2 + q \geq 0$.

Solving Eq. (1) rigorously for decoding is computationally hard in general cases. However, one can construct a practical decoding algorithm based on the belief propagation (BP) [7] or the Thouless-Anderson-Palmer (TAP) approach [12]. It has recently been shown that these two frameworks provide the same algorithm in the case of ECC [3]. This is also the case under the current context. For distribution (11), the algorithm derived from the BP/TAP frameworks becomes as

$$\begin{aligned} m^1_{\mu i} &= \frac{a_{\mu i} + m_1 + m_2 a_{\mu i} b_i + q b_i}{1 + m_1 a_{\mu i} + m_2 b_i + q a_{\mu i} b_i}, \quad m^2_{\mu i} = \frac{b_{\mu i} + m_2 + m_1 a_i b_{\mu i} + q a_i}{1 + m_1 a_i + m_2 b_{\mu i} + q a_i b_{\mu i}}, \\ \widehat{m}^1_{\mu i} &= u_\mu \prod_{j \in \mathcal{L}_1(\mu)/i} m^1_{\mu j}, \quad \widehat{m}^2_{\mu i} = v_\mu \prod_{j \in \mathcal{L}_2(\mu)/i} m^2_{\mu j}, \end{aligned} \tag{12}$$

where we denote $a_{\mu i} \equiv \tanh \sum_{\nu \in \mathcal{M}_1(i)/\mu} \tanh^{-1} \widehat{m}^1_{\nu i}$ and $a_i \equiv \tanh \sum_{\mu \in \mathcal{M}_1(i)} \tanh^{-1} \widehat{m}^1_{\mu i}$, and similarly for b's. Here, $\mathcal{M}_1(i)$ and $\mathcal{M}_2(i)$ indicate the set of all indices of nonzero components in the ith column of the sparse matrices A and B, respectively. Eq. (12) can be solved iteratively from the appropriate initial conditions. After obtaining a solution, approximated posterior means can be calculated for $i = 1, 2, \ldots, N$ as

$$m^1_i = \langle S_i \rangle = \frac{a_i + m_1 + m_2 a_i b_i + q b_i}{1 + m_1 a_i + m_2 b_i + q a_i b_i}, \quad m^2_i = \langle \tau_i \rangle = \frac{b_i + m_2 + m_1 a_i b_i + q a_i}{1 + m_1 a_i + m_2 b_i + q a_i b_i}, \tag{13}$$

which provide an approximation to the Bayes-optimal estimators as $\xi_i = \mathrm{sign}(m^1_i)$ and $\eta_i = \mathrm{sign}(m^2_i)$, respectively.

In order to investigate the efficacy of the current method for finite C_1 and C_2, we have numerically solved Eqs. (5) and (12) for $K_1 = K_2 = 6$ and $C_1 = C_2 = 3$ ($R_1 = R_2 = 1/2$), results of which are summarized in Fig. 2. Numerical results for the saddle point equation (5) were obtained by an iterative method using $10^4 - 10^5$ bin models for each probability distribution. $10 - 10^2$ updates were sufficient for convergence in most cases. Similarly to the case of $C_1,\ C_2 \to \infty$, there can be four types of solutions corresponding to combinations of decoding success and failure on the two sources. The obtained phase diagram is quite similar to that for $C_1,\ C_2 \to \infty$. This implies that the current compression code *theoretically* has a good performance close to the optimal one that is saturated in the limit $C_1,\ C_2 \to \infty$ although the choice of $C_1 = C_2 = 3$ is far from such limit.

However, this does not directly mean that the suggested performance can be obtained *in practice*. Since the variables are updated locally in the BP/TAP decoding algorithm (12), it may become difficult to find the thermodynamically dominant state when there appear suboptimal states which have large basins of attraction. This suggests that the practical performance for the perfect decoding is determined by the spinodal points of the suboptimal states similarly to the case of ECC [6]. In order to confirm this conjecture, we have numerically compared the practical limit of the perfect decoding obtained by the BP/TAP decoding algorithm (12) and the spinodal points of the non-FF solutions. These two results exhibit an excellent consistency supporting our conjecture. In the figure, the perfectly decodable region obtained by the BP/TAP algorithm for $m_1 = 0.7$ cases is indicated as the area surrounded by the spinodal points and the boundaries for the feasible region $1 + 0.7 - m_2 - q = 0$ and $1 + 0.7 + m_2 - q = 0$. This looks narrow compared to the theoretical limit, which might provide a negative impression on the practical utility of this code. Nevertheless, we still consider that the current method may be practically useful because the size of information that can be represented by parameters in the region is not so small as what the area looks.

In summary, we have developed an efficient method of data compression in a multi-terminal communication network, taking advantage of the sparse matrix based linear compression

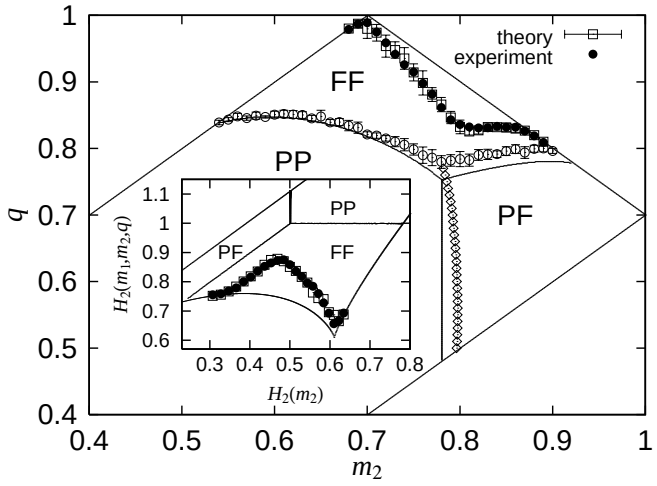

Fig. 2 – Phase diagram for $K_1 = K_2 = 6$ and $C_1 = C_2 = 3$ code in the case of component-wise correlated information source (11). This figure shows that the feasible region in $m_2 - q$ plane for $m_1 = 0.7$ is classified into three states. Phase boundaries obtained by numerical methods are indicated by $\circ$ with errorbars (FF/PP and FF/PF) and $\diamond$ (PF/PP). These are close to those for $K_1 = K_2 \to \infty, C_2 = C_2 \to \infty$ (curves and the vertical line). Practically decodable limits of the TAP/BP algorithm obtained for $N = 10^4$ systems are indicated as $\bullet$. These are well evaluated by the spinodal points of non-FF solutions ($\Box$ with errorbars). Inset: The practical limits are represented by the sizes of transmitted information. The horizontal and vertical axes show the entropy of the second source $\boldsymbol{\tau}$ and the joint entropy, respectively.

codes. We observed several practical properties of the codes of this type in the simplest model of a data compression employed for a network communication proposed by SW. Studying the typical performance of the linear compression codes in a network, which complements the methods used in the information theory literature, is the first step towards understanding typical properties of the network based systems.

* * *

The author thanks Y. Kabashima and T. Ohira for valuable discussions and suggestions. This work was partly supported by the Japan Society for the Promotion of Science.

REFERENCES

[1] COVER T.M. and THOMAS J.A., *Elements of Information Theory* (Wiley, NY) 1991.
[2] GALLAGER R. G., *IRE Trans. Inf. Theory*, **IT-8** (1962) 21.
[3] KABASHIMA Y. and SAAD D., *Europhys. Lett.*, **44** (1998) 668.
[4] MACKAY D. J. C., *IEEE Trans. Inf. Theory*, **45** (1999) 399.
[5] MONTANARI A., (2001), cond-mat/0104079.
[6] MURAYAMA T., KABASHIMA Y., SAAD D. and VICENTE R, *Phys. Rev. E*, **62** (2000) 1577.
[7] PEARL J., *Probabilistic Reasoning in Intelligent Systems:* Network of Plausible Inference (Morgan Kaufmann, SF) 1988.
[8] RICHARDSON T., SHOKROLLAHI A. and URBANKE R. , "Design of provably good low density parity check codes" (1999), preprint.

[9] Shannon C. E., *Bell Syst. Tech. J.*, **27** (1948) 379.
[10] Slepian D. and Wolf J. K., *IEEE IT*, **19** (1973) 471.
[11] Sourlas N., *Nature*, **339** (1989) 693.
[12] Thouless D.J., Anderson P.W. and Palmer R.G., *Phil. Mag.* , **35** (1977) 593.
[13] Wong K. Y. M. and Sherrington D., *J. Phys. A*, **20** (1987) L793.
[14] Ziv J. and Lempel A., *IEEE Trans. Info. Theory*, **23** (1977) 337.